



# Retention and release of deuterium implanted in W and Mo

S. Nagata \*, K. Takahiro, S. Horiike, S. Yamaguchi

*Institute for Materials Research, Tohoku University, Katahira 2-1-1, Aoba-ku Sendai, 980-8577, Japan*

---

## Abstract

Retention and thermal release of deuterium implanted in W with various carbon contents were studied by ion beam analysis techniques. The correlation between implantation induced defects and deuterium trapping in W was examined in comparison with that in Mo. The D concentration in the near surface layer of the W crystal was higher than that in the Mo crystal during 10 keV D<sub>2</sub><sup>+</sup> implantation at room temperature. In case of the D implanted Mo crystal, the isolated interstitial atoms were mainly recognized by the ion channeling. On the other hand, a large lattice distortion caused by the extended defects was observed in the near surface layer of the D implanted W at room temperature, and the distortion was not effectively formed above 390 K. The appreciable amount of the retained D atoms was released from pure W at around 450 K at which the lattice distortion was partly annealed out. The thermal release of D retained in the carbon containing W abruptly occurred at about 350 K, independent of the carbon contents. © 1999 Elsevier Science Inc. All rights reserved.

*Keywords:* Carbon; Defect; Deuterium depth profiling; Deuterium irradiation; Molybdenum; Tungsten

---

## 1. Introduction

The high-Z materials such as tungsten, molybdenum and their carbides are considered as candidate materials for the plasma facing components in fusion devices. Hydrogen trapping and release properties of the first wall materials are important for determining the tritium inventory and for controlling the particle balance in the plasma.

Previous studies on Mo and W have shown that radiation induced defects act as trapping sites for hydrogen and play an important role for retention properties in the near surface layer [1–3]. Furthermore, the retention, thermal desorption and re-emission of hydrogen implanted in Mo and W strongly depend on the microstructure of specimens prepared by different methods [4,5], and the impurity such as carbon and carbides which would be formed on the surface of the plasma facing materials during the operation of the fusion machine [6,7]. These experimental results indicate that the irradiation induced defects, impurities and lattice im-

perfections are essential for the hydrogen trapping. However, the data base for the hydrogen in W and Mo under the fusion environment is still limited [8], and the mechanism of the hydrogen trapping and release in W and Mo and their carbides is not well understood.

In the present work, the retention and thermal release behaviour of deuterium implanted in W and Mo was studied in detail in connection with the implantation induced defects as well as the carbon content of the specimens. Ion beam analysis techniques were applied for depth profiling of the retained deuterium implanted in the samples and for the study of damage produced by the D ion implantation.

## 2. Experimental

Specimens used were  $\langle 111 \rangle$  oriented single crystals of W, Mo and polycrystalline foils (99.95%) of 25  $\mu\text{m}$  thickness. A single crystal of W prepared by floating zone melting methods were cut into disks of 8 mm diameter and 0.5 mm thickness, followed by electropolishing in 0.1 N NaOH solution. The polycrystalline foils fabricated by powder metallurgy were annealed at 1500 K for 2 h in  $10^{-8}$  Pa vacuum prior to the deuterium

---

\* Corresponding author. Tel.: +81-22 215 2058; fax: +81-22 215 2061; e-mail: nagata@wani.imr.tohoku.ac.jp.

implantation. In order to make carbonized layer on the specimen, a carbon film was kept in contact with the surface of the metal foil during the heat treatment as described above. The chemical composition of the carbon containing layer was determined by the backscattering spectroscopy. In addition to the W crystal, the Mo crystal was also examined for comparison; the preparation procedure has been described elsewhere [9]. The specimen was placed on a heatable sample holder in a scattering chamber connected to a 1.7 MV tandem accelerator. The implantation of D ions was carried out by using a 10 keV ion gun with a velocity filter placed at an angle of  $40^\circ$  to the analyzing beam. The D ion implantation was carried out along the surface normal, which was about  $10^\circ$  from the  $\langle 111 \rangle$  axis of the single crystal, with a flux density of about  $1 \times 10^{18}$  D ions/m<sup>2</sup> at a temperature range between 300 and 520 K.

Concentration profiles of D atoms in the near surface region of the specimen were measured by the elastic recoil detection (ERD) technique. A <sup>4</sup>He ion beam of 2.8 MeV energy was incident on the specimen at an angle of  $75^\circ$  to the surface normal and the recoiled D atoms were detected at the angle of  $25^\circ$  with respect to the analyzing beam. An Al foil of 12  $\mu$ m thickness was placed in front of the detector to absorb the scattered <sup>4</sup>He ions from the specimen. The depth resolution of the present ERD experiments was estimated to be about 25 nm at the surface of W and Mo. Because all specimens had smooth surface, the depth resolution due to the surface roughness was expected to be minimized and no difference of the depth resolution was expected among the various samples. To study the lattice disorder produced by the D ion implantation, the channeling experiments along the  $\langle 111 \rangle$  axis were performed using the backscattering of <sup>4</sup>He ions with an incident energy of 0.5 to 2.8 MeV. Thermal release of the retained D atoms and annealing of the implantation induced damage were measured after each stage of isochronal annealing for 600 s in the temperature range from 300 to 870 K.

### 3. Results and discussion

Fig. 1 shows the concentration depth profiles of D atoms retained in the near surface region for three kinds of the W specimens and a Mo single crystal after the implantation with 10 keV D<sub>2</sub><sup>+</sup> at the dose of about  $1 \times 10^{22}$  D/m<sup>2</sup> at room temperature. The D depth profiles in W specimens extends to a depth more than 100 nm, which was much larger than the defect distribution calculated by TRIM-code [10]. Especially for the carbon containing W foil, much higher concentration of D atoms was retained at the large depth, although no significant difference of the maximum concentration is observed in the specimens having different microstructure and carbon contents. For the pure W foil in which

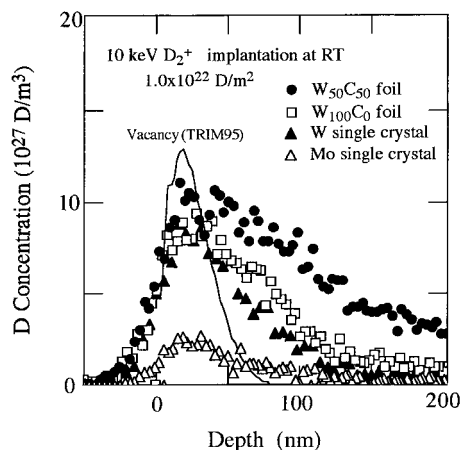


Fig. 1. Concentration depth profiles of D atoms in the near surface region of three kinds of the W specimens and a Mo single crystal after the implantation with 10 keV D<sub>2</sub><sup>+</sup> at a dose of about  $1 \times 10^{22}$  D/m<sup>2</sup> at room temperature.

the D concentration was slightly higher than that in the single crystal W, a large part of the defects such as dislocations formed during the fabrication process seemed to be annealed out by heat treatment at 1500 K for 2 h. On the other hand, deuterium trapping was probably affected by impurities of carbon or carbide materials formed in the W foil.

In comparison with the Mo crystal, the similar shapes of the retained D profiles were observed for W single crystals. But, the saturation concentration of D in the W single crystal at room temperature was several times higher than that in the Mo crystal. The larger retention of D in W at room temperature in comparison with Mo was also found by the thermal desorption measurements of Haasz and Davis [11] with 1 keV D ion implantation.

The backscattering spectra of 1 MeV He aligned for  $\langle 111 \rangle$  axial direction in the D implanted Mo and W crystals are shown in Fig. 2 as a function of depth. The D implantation was made with 10 keV D<sub>2</sub><sup>+</sup> at a dose of about  $2 \times 10^{22}$  D/m<sup>2</sup> at room temperature. The aligned yields are normalized as dechanneled yields  $\chi_D$  defined as the ratio of the aligned yield to the random yield. The dechanneled yields for the unimplanted crystals were identical for both Mo and W crystals with the value of 0.02. In the backscattering spectrum for the D implanted Mo crystal, a sharp peak was observed in the near surface. This peak originates from the He ion scattered by single collision with the target atoms displaced from the lattice site, and indicates the existence of interstitial (displaced) Mo atoms produced by the D implantation. Hereafter, we denote the displaced atoms which produce the direct scattering as the interstitial atoms. The disordered region was concentrated on the near surface layer of 0–20 nm depth and was consistent with the

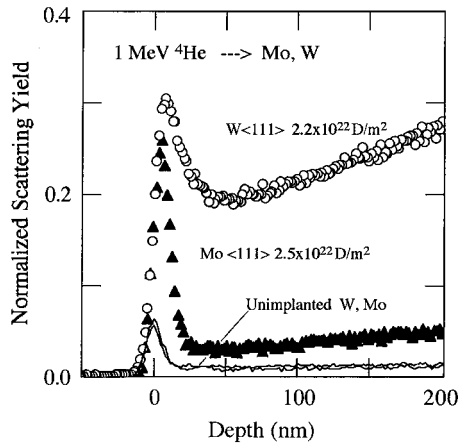


Fig. 2. Backscattering yield versus depth for 1 MeV He incident along the  $\langle 111 \rangle$  axial direction in Mo ( $\blacktriangle$ ) and W ( $\circ$ ) crystals after the implantation with 10 keV  $D_2^+$  at a dose of about  $2 \times 10^{22}$  D/m<sup>2</sup> at room temperature.

defect distribution expected by the TRIM calculation as shown in Fig. 1. The number of the interstitial Mo atoms was estimated to be about  $1 \times 10^{20}$  atoms/m<sup>2</sup> which is nearly the same value of the retained D atoms.

In the W crystal, however, a broader peak followed by a large dechanneled yield beyond the implant depth appeared in the backscattering spectrum. The peak originates from single collision with interstitial W atoms produced by D implantation as the same as observed in the Mo crystal. On the other hand, the large dechanneled yield beyond the peak could be attributed to the multiple scattering by the extended defects such as dislocation loops, which accompany the extensive lattice distortion around the defects. The observed dechanneled yield below the peak region for the D implanted crystal can be expressed by the number of defects in the path of the analyzing  $^4\text{He}$  ion beam as follows [12]:

$$[1 - \chi_D(z)]/[1 - \chi_V(z)] = \exp[-\sigma N(z)], \quad (1)$$

where,  $\chi_D(z)$  and  $\chi_V(z)$  are dechanneled yields obtained from a damaged and an unimplanted crystal, respectively,  $\sigma$  is the dechanneling cross section for the defects and  $N(z)$  is the total number of defects per unit area integrated from the surface to the depth of  $z$ . The dechanneling cross section for the interstitial type defects is inversely proportional to the incident energy. In the case of dechanneling by dislocations [13] Eq. (1) is rewritten as

$$[1 - \chi_D(z)]/[1 - \chi_V(z)] = \exp[-\lambda L(z)], \quad (2)$$

where  $L(z)$  denotes the total length of dislocation line between the surface and the depth of  $z$ ,  $\lambda$  is the dechanneling cross section per unit length, and  $\lambda L(z) = -\ln\{[1 - \chi_D(z)]/[1 - \chi_V(z)]\}$  is defined as the dechanneling parameter. On the contrary to the dechanneling

due to single scattering by interstitial atoms, the dechanneling cross section by the dislocation line is known to be proportional to  $E^{1/2}$  [13], and the relation is expressed as

$$\lambda(z) = k(z)E^{1/2}, \quad (3)$$

where the parameter  $k$  depends on the channeled particle and the target atoms. This energy dependence of the dechanneling cross section can be applied for the dislocation loop, if the dechanneling cross section is less than the loop radius [14]. In Fig. 3, the dechanneling parameter at the depth of 100 nm for W  $\langle 111 \rangle$  were plotted as a function of the incident  $^4\text{He}$  energy. The implantation was carried out at 300, 390, and 520 K up to a dose of  $1.4 \times 10^{22}$  D/m<sup>2</sup>. The dechanneling parameter increases with increasing the ion energy except for the implantation at 520 K, and the magnitude of the dechanneling parameter drastically decreased for implantation at 390 K and above. It may be concluded from this result that the large amount of the extended defects such as dislocation loops and dislocation network were formed in the W crystal by the D implantation below 400 K. The lattice distortion created by the implantation at room temperature was not completely annealed out at 700 K, although very little distortion was detected for the implantation at 520 K.

The dechanneling cross section  $\lambda$  is theoretically estimated to be about 1 nm for channeling of W  $\langle 111 \rangle$  with 1 MeV  $^4\text{He}$  [15], and the parameter  $k$  is evaluated to be  $0.2 \text{ MeV}^{-1/2}$  from the energy dependence of the dechanneling parameter at 300 K. The total dislocation

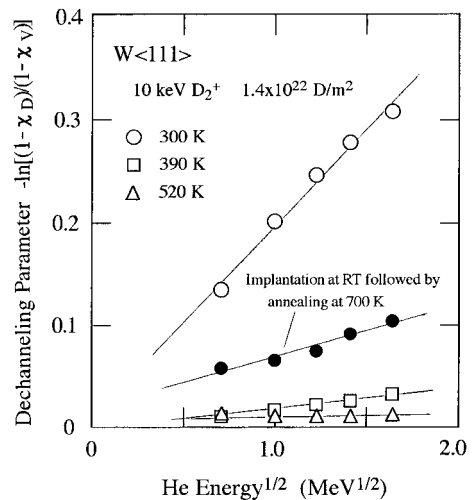


Fig. 3. Dechanneling parameter on W  $\langle 111 \rangle$  for the D implantation at 300 K ( $\circ$ ), 390 K ( $\square$ ) and 520 K ( $\triangle$ ) plotted as a function of the incident  $^4\text{He}$  energy. Closed circles ( $\bullet$ ) indicate the parameter obtained for the specimen annealed at 700 K for 30 min after the D implantation at 300 K.

length is calculated as  $L = 2 \times 10^8 \text{ m}^2$ . The defect density at 300 K implantation is estimated to be  $2 \times 10^{15} / \text{m}^2$  from the total dislocation length divided by the distorted layer thickness of 100 nm. The estimated value of the dislocation density are comparable with the previous TEM measurements of dislocation loop density in the W crystals bombarded by 8 keV hydrogen ion [16]. The defect density decreased to  $2 \times 10^{14} / \text{m}^2$  at 390 K because the parameter  $k$  was reduced to about  $0.02 \text{ MeV}^{-1/2}$ .

In Fig. 4, the dose dependence of the D retention in the near surface layer (0–100 nm) of the W crystals at three different temperature is compared with that of the dechanneling parameters obtained for the  $\langle 111 \rangle$  orientation. At room temperature, the dose dependence of the retained D atoms was similar to that of the dechanneling parameter whose amplitude corresponds to the amount of the extended defects. The correlation between the D retention and the implantation induced lattice distortion in the W crystals supported by the result that the D retention increased with the accumulation of the extended defects during the D implantation.

For the implantation at 390 K, the dechanneling parameter was reduced to a very small value, but the appreciable amount of the D atoms was still retained in the near surface layer of the W crystal as seen in Fig. 4. According to the depth profiling, the D atoms were retained only in the shallow depth of less than 100 nm at and above 390 K, whereas at room temperature they were distributed to the depth more than 100 nm, as

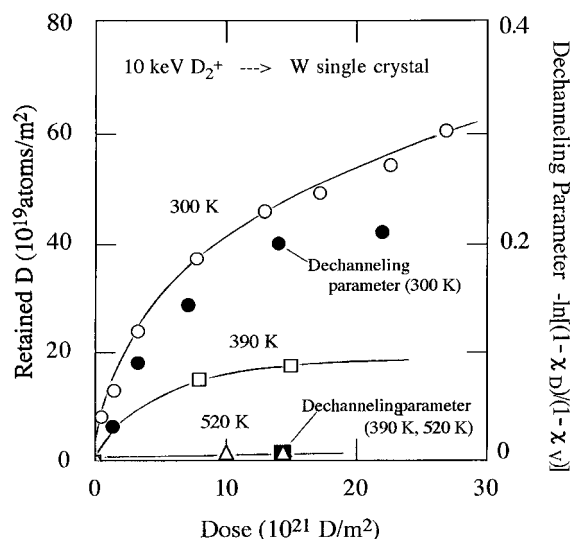


Fig. 4. D retention in the near surface layer of W single crystals as a function of the D implantation dose at 300 K (○), 390 K (□) and 520 K (△), together with the dechanneling parameters obtained by 1 MeV  $^4\text{He}$  beam for the  $\langle 111 \rangle$  orientation at 300 K (●), 390 K (▲) and 520 K (■).

shown in Fig. 1. In the channeling experiments, the scattering yields from the interstitial atoms appeared as a sharp peak in the aligned spectrum as seen in Fig. 2. The number of those interstitial atoms was almost unchanged with the implantation temperature. Therefore, at higher temperature, the lattice distortion was not effectively formed particularly at the large depth, and the trapping of D atoms is considered to be more associated with vacancy type defects created in the shallow depth where interstitial atoms were detected by the ion channeling experiments. The amount of retained D was very small at the near surface and nearly no D was found in depth larger than 100 nm for the implantation at 520 K. This temperature dependence of the D retention in the W crystal is consistent with the results obtained by thermal desorption experiments [17].

The D retention in the near surface layer of the W crystal after the isochronal annealing of 10 min at each temperature is shown in Fig. 5, together with the number of interstitial atoms and dechanneling parameters. Each value is normalized by the value obtained after the implantation up to the dose of  $1.4 \times 10^{22} \text{ D/m}^2$  at 300 K. The error for the estimated number of interstitial atoms is large, because direct scattering yields from isolated interstitial atoms superimposed on the dechanneling contribution from extended defects. As seen in Fig. 5, the release of D atom atoms from the W crystal occurred mainly between 350 and 500 K. No significant difference was observed between the thermal release of D atoms retained in a heavily damaged layer (0–100 nm) and that at the greater depth (100–300 nm). The deuterium trapping seems to be identical in the heavily damaged layer and at the greater depth where the defect density

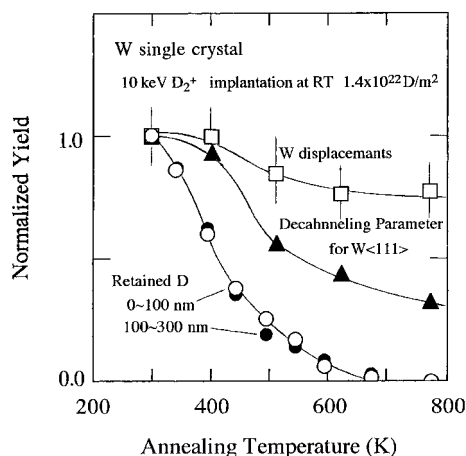


Fig. 5. Normalized D retention in the near surface layer (0–100 nm: ○) and in the deeper depth (100–300 nm: ●) of the W crystal versus annealing temperature, together with the normalized values of the number of the interstitial atoms (□) and dechanneling parameters (▲).

estimated by the ion channeling was considerably smaller than that at the depth of less than 100 nm. The change of the dechanneling parameter indicates that a half of the extended defects produced by the D implantation at room temperature recovered at the temperature 500 K, but 30% of them still remained at 800 K. Dislocation loops created with low implantation dose at room temperature were recovered by slip motion to the surface during the isochronal annealing, and almost vanished at about 600 K [16]. The disappearance of the dislocation loops might be prevented in the present experiments by higher implantation dose because of large accumulation of defects in the implanted surface layer. In comparison with the recovery of the lattice distortion, the observed direct scattering yield slowly decreased with the increase of the annealing temperature. About 80% of the interstitial W atoms created by the D implantation at room temperature was still detected at 800 K.

The D retention in the implant surface layer of various kinds of W samples is shown in Fig. 6 as a function of annealing temperature. The D retention for the pure W foil at each temperature was higher than that for the single crystal. This can be related to the difference of the recovery of defects in each specimen. Because the dislocation loops in the single crystal W is expected to move more easily to the surface than in the foil material fabricated by powder metallurgy [16], radiation induced defects might recover at lower annealing temperature in comparison to the foil material. Consequently, the release of retained D atoms from the single crystal occurs at lower annealing temperature. The defect accumulation during the D implantation might occur effectively in the foil material. It is consistent with a slightly larger D retention in the foil than that in the single crystal W as shown in Fig. 1.

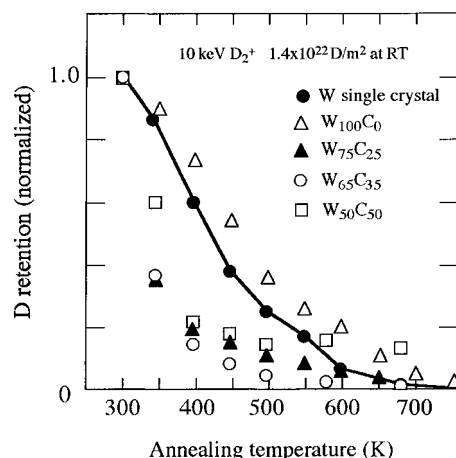


Fig. 6. Normalized D retention in the near surface layer of the W crystal and the W foils having various carbon content as a function of annealing temperature.

On the other hand, the release behaviour of D for carbon containing W foils was quite different from that for pure W as seen in Fig. 6. The release of D atoms occurred mainly at 350 K, and no significant release was observed at higher temperature. The release behaviour was almost the same for samples with different composition of carbon. In the case of W<sub>50</sub>C<sub>50</sub> specimen, a little fraction of deuterium was still retained at the temperature up to 700 K. The D retention above 700 K might be due to the trapping by precipitates of graphite materials in the carbonized layer. The release at lower temperature compared to the pure crystal was observed for the Mo crystal whose surface layer was enriched with carbon [7]. However, the mechanism of the deuterium retention in the carbon contained W and Mo is not known. Further experiments are necessary to clarify the carbon effect on the retention and release of deuterium in W and Mo.

#### 4. Conclusion

The trapping and thermal release of D atoms implanted in W and Mo in connection with the defects created by the D implantation and the carbon content of the specimens were studied by the ion beam analysis techniques.

The D retention in the near surface of the W crystal was several times higher than that in the Mo crystal at room temperature. In the ion channeling experiments, the large lattice distortion was observed for the W crystal during the 10 keV D<sub>2</sub><sup>+</sup> implantation, whereas the isolated interstitial atoms were mainly detected for the Mo crystal. The results indicate that the extended defects such as dislocation loops and stacking faults created by D implantation play an important role for trapping of D atoms in the W crystal at room temperature. The defect accumulation and the D retention in the W crystal strongly depends on the implantation temperature. The lattice distortion was not effectively formed in the W crystal under the implantation at 520 K, even with a dose of  $1 \times 10^{22}$  D/m<sup>2</sup>, and the amount of retained D was by a factor of about 30 smaller than that for room temperature.

The amount of retained D atoms in the near surface of the carbon containing W foil is larger than that in pure W specimens at room temperature. On the other hand, the thermal release of D retained in the W foils with various carbon contents occurred abruptly at about 350 K which is considerably lower than that for the pure W and graphite.

#### References

- [1] J. Böttiger, S.T. Picraux, N. Rud, T. Laursen, J. Appl. Phys. 48 (1977) 920.
- [2] S.M. Myers, F. Besenbacher, J. Appl. Phys. 60 (1986) 3499.

- [3] T. Tanabe, N. Hachino, M. Takeo, *J. Nucl. Mater.* 176&177 (1990) 666.
- [4] V.Kh. Alimov, B.M.U. Sherzer, *J. Nucl. Mater.* 240 (1996) 75.
- [5] C. Garcia-Rosales, P. Franzen, H. Plank, J. Roth, E. Gauthier, *J. Nucl. Mater.* 233–237 (1996) 803.
- [6] W. Wang, V.Kh. Alimov, B.M.U. Scherzer, J. Roth, *J. Nucl. Mater.* 241–243 (1997) 1087.
- [7] S. Nagata, K. Takahiro, S. Yamaguchi, *J. Nucl. Mater.* 258–263 (1998) 907.
- [8] P. Franzen, C. Garcia-Rosales, H. Plank, V.K. Alimov, *J. Nucl. Mater.* 241–243 (1997) 1082.
- [9] S. Nagata, T. Hasunuma, K. Takahiro, S. Yamaguchi, *J. Nucl. Mater.* 248 (1997) 9.
- [10] J.P. Biersack, L.G. Haggmark, *Nucl. Instrum. Meth.* 174 (1980) 257.
- [11] A.A. Haasz, J.W. Davis, *J. Nucl. Mater.* 241–243 (1997) 1076.
- [12] E. Rimini, in: J.P. Thomas, A. Cachard (Eds.), *Material Characterization Using Ion Beams*, Plenum, New York, 1978, p. 455.
- [13] S.T. Picraux, E. Rimini, G. Foti, S.U. Campisano, *Phys. Rev. B* 18 (1978) 2078.
- [14] H. Kudo, *Phys. Rev. B* 18 (1978) 5995.
- [15] J. Mory, Y. Quéré, *Radiat. Eff.* 13 (1972) 13.
- [16] R. Sakamoto, T. Muroga, N. Yoshida, *J. Nucl. Mater.* 220–222 (1995) 819.
- [17] R. Sakamoto, T. Muroga, N. Yoshida, *J. Nucl. Mater.* 233–237 (1996) 776.